

This discussion paper is/has been under review for the journal Hydrology and Earth System Sciences (HESS). Please refer to the corresponding final paper in HESS if available.

Evaluation of the JULES land surface model in simulating catchment hydrology in Southern Africa

N. C. MacKellar¹, S. J. Dadson², M. New^{1,2}, and P. Wolski³

¹African Climate and Development Initiative, University of Cape Town, Private Bag X3, Rondebosch 7701, South Africa

²School of Geography and the Environment, University of Oxford, South Parks Road, Oxford, OX1 3QY, UK

³Climate Systems Analysis Group, University of Cape Town, Private Bag X3, Rondebosch 7701, South Africa

Received: 10 July 2013 – Accepted: 28 July 2013 – Published: 22 August 2013

Correspondence to: N. C. MacKellar (neil@csag.uct.ac.za)

Published by Copernicus Publications on behalf of the European Geosciences Union.

11093

Abstract

Land surface models (LSMs) are advanced tools which can be used to estimate energy, water and biogeochemical exchanges at regional scales. The inclusion of a river flow routing module in an LSM allows for the simulation of river discharge from a catchment and offers an approach to evaluate the response of the system to variations in climate and land-use, which can provide useful information for regional water resource management. This study offers insight into some of the pragmatic considerations of applying an LSM over a regional domain in Southern Africa. The objectives are to identify key parameter sensitivities and investigate differences between two runoff production schemes in physically contrasted catchments. The Joint UK Land Environment Simulator (JULES) LSM was configured for a domain covering Southern Africa at a 0.5° resolution. The model was forced with meteorological input from the WATCH Forcing Data for the period 1981–2001 and sensitivity to various model configurations and parameter settings were tested. Both the PDM and TOPMODEL sub-grid scale runoff generation schemes were tested for parameter sensitivities, with the evaluation focussing on simulated river discharge in sub-catchments of the Orange, Okavango and Zambezi rivers. It was found that three catchments respond differently to the model configurations and there is no single runoff parameterization scheme or parameter values that yield optimal results across all catchments. The PDM scheme performs well in the upper Orange catchment, but poorly in the Okavango and Zambezi, whereas TOPMODEL grossly underestimates discharge in the upper Orange and shows marked improvement over PDM for the Okavango and Zambezi. A major shortcoming of PDM is that it does not realistically represent subsurface runoff in the deep, porous soils typical of the Okavango and Zambezi headwaters. The dry-season discharge in these catchments is therefore not replicated by PDM. TOPMODEL, however, simulates a more realistic seasonal cycle of subsurface runoff and hence improved dry-season flow.

11094

1 Introduction

As global- and regional scale climate models have become increasingly complex, their schemes to represent exchanges of energy and water at the earth's surface have developed into detailed land surface models (LSMs). These LSMs have evolved to include explicit representations of energy, water and trace gas exchanges between land and atmosphere. Subsurface vertical fluxes of water and heat, as well as horizontal runoff, are calculated in a multilayer soil column. The biosphere is typically represented in terms of vegetation structure, physiology and phenology, as well carbon cycling. Because of the relatively coarse grid resolution at which climate models typically operate, methods have been introduced to account for sub-grid-scale heterogeneities. For improved representation of runoff in LSMs, sub-grid-scale runoff generation schemes have been implemented (e.g. Gedney and Cox, 2003; Clark and Gedney, 2008). To simulate streamflow in river catchments, runoff routing schemes are also now widely used (e.g. Miller et al., 1994; Hagemann and Dümenil, 1998; Oki et al., 1999; Alkama et al., 2010; Dadson et al., 2011).

The capabilities of a LSM in simulating catchment-scale hydrology are thus comparable to a stand-alone distributed hydrological model, but the implementation of these two suites of modelling tools and the spatial scales at which they are applied tend to be somewhat different. Whereas a stand-alone hydrological model is typically applied to a specific catchment, a LSM usually has a spatial coverage matching that of a climate or earth-system model – such as full global coverage with a grid resolution of 100–300 km, or a continental domain with 25–50 km resolution. The LSM can be run as a fully coupled component of the earth-system model, or run in an off-line mode where input is provided by climate model output or a gridded observational product. The standard approach to configure a stand-alone hydrological model is to calibrate it to the target catchment by tuning model parameters against observations such that the simulated output closely matches observed flow. This has the advantage of reducing model bias, but calibration procedures are not without caveats and are limited by the

11095

availability and quality of observational records. Furthermore, calibration procedures that result in a single optimal solution tailored to a particular calibration period do not represent a possible range of equally likely model solutions. This problem of so-called equifinality, which accounts for the possibility that a model may have multiple acceptable outcomes is discussed in detail by Beven and Freer (2001) and Beven (2006). An alternative approach for determining model parameters is to employ a reduced parameter model where parameters are estimated a priori from relationships to measured physical properties such as soil characteristics or topography. It is the latter approach that is better suited to the application of a LSM at a global or regional scale, where, given diversity in the physical characteristics of river catchments within the domain, a globally-calibrated model is likely to be unrepresentative of the full domain. It would also be impractical to perform individual calibration for different catchments or subsets of the domain, particularly if such calibration involved overcompensation for deficiencies in other components of the land-surface model.

Most of Southern Africa is a water-stressed region where water consumption is high compared to available supply (Meigh et al., 1999; Vörösmarty et al., 2000). This is compounded by high inter- and intra-annual variability in mean annual runoff (MAR) in the region (Schulze, 2000), which makes the management of water resources particularly challenging and is also likely to make the detection of a long-term climate change signal very difficult. Furthermore, de Wit and Stankiewicz (2006) show that most of Southern Africa falls within an unstable regime where perennial drainage responds to changes in rainfall in a non-linear manner, such that a change in rainfall can lead to a greatly amplified drainage response where a threshold is crossed. Analysis of projections of both climate and population changes for the 21st century indicates a general likelihood of increased water stress in the region (Arnell, 2004). Given this critical state, an improved understanding of the linkages between climate and hydrology in the region will be greatly beneficial. The aim of this work is therefore to configure and test a land-surface modelling system over Southern Africa as a tool to further this understanding. The approach taken is to offer insight into some of the pragmatic considerations of

11096

applying an LSM over a regional domain and specific attention is paid to the simulation of river discharge (Q) and evapotranspiration (ET) at monthly timescales for sections of the Orange, Okavango and Zambezi catchments. The objective is not to perform a thorough tuning or optimization procedure, but rather to test the model's sensitivities to various parameters and to investigate differences between two runoff production schemes in physically contrasted catchments in order to assess the potential applicability of the model to investigate hydrological processes in the region. The use of two runoff production schemes offers an opportunity to evaluate whether one offers a consistent advantage over the other, or if their relative performance is catchment-dependant.

2 Models, data and method

2.1 JULES LSM

The LSM used in this study is the Joint UK Land Environment Simulator (JULES). The model is described in detail by Best et al. (2011), Clark et al. (2011) and Essery et al. (2003), but a brief overview of the relevant hydrological components is given here. JULES is evolved from the Met Office Surface Exchange Scheme (MOSES; Cox et al., 1999), which is the LSM used within the UK Met Office's suite of global and regional climate models. JULES can therefore be used in a stand-alone model, or fully coupled to a climate model.

For surface exchanges of water, JULES includes explicit formulations for canopy storage, throughfall, infiltration, surface runoff, plant transpiration and evaporation from bare soil and open water stores. In the current setup, soil hydraulics are represented by the scheme of Brooks and Corey (1964). Super-saturation in soil layers is treated such that if a layer reaches saturation point, further input of water from above is routed down the soil column where, if the lowest layer is saturated, it is added to subsurface runoff. Sub-grid-scale heterogeneities in the soil column are not explicitly accounted for

11097

in JULES, but heterogeneity in soil moisture store depths is introduced by implementing either the PDM or TOPMODEL parameterization schemes, as outlined below.

The Probability Distributed Model (PDM; Moore, 1985) is a conceptual model in which sub-grid soil stores of varying capacity are distributed within a grid-box according to a probability distribution function (pdf). When a soil store becomes saturated during a rainfall event it will begin to contribute to the fraction of the grid-box that is producing surface runoff. The saturated fraction of a grid box is given as

$$f_{\text{sat}} = 1 - \left[1 - \frac{\theta}{\theta_{\text{sat}}} \right]^{\frac{b}{b+1}} \quad (1)$$

(Best et al., 2011) where θ is actual soil water content, θ_{sat} is soil water content at saturation and b is a shape parameter which determines the relative proportion of shallower to deeper stores. A higher value of b results in fewer high capacity ("deep") stores relative to low capacity ("shallow") stores and so will result in a more rapid production of surface runoff.

In TOPMODEL (Beven and Kirkby, 1979; Beven et al., 1995; Beven, 1997), a topographical index, λ , is defined as $\ln(a/\tan(\beta))$, where a is the area draining to this point per unit contour length and $\tan(\beta)$ is the slope of the land surface. Unlike the representation of soil stores in PDM, which is not related to any physical characteristics of the catchment, λ has some physical meaning and can be derived from a digital elevation model (DEM). Sub-grid variation in λ is modelled using a gamma distribution. A critical value for the topographical index, which is calculated from moisture conditions in the soil profile, is used to define the surface fraction of a grid-box that is saturated. This saturated fraction produces saturation-excess overland flow. Gedney and Cox (2003) implemented TOPMODEL in JULES with an additional storage layer beneath the standard 4-layer, 3 m deep soil column and a prognostically modelled grid-box-mean water table depth. In the zone beneath the standard 4 layers, saturated conductivity, K_{sat} , is assumed to decrease exponentially with depth according to

$$K_{\text{sat}}(z) = K_{\text{sat}}(0) \exp(-fz) \quad (2)$$

11098

where z is depth, $K_{\text{sat}}(0)$ is saturated conductivity at the top of the layer and f is an exponent defining the rate of decay of saturated conductivity with depth (Gedney and Cox, 2003). Subsurface runoff is generated from any soil layer below or containing the top of the water table. When the water table intersects with the land surface, saturation-excess overland flow is produced. It is assumed that the gradient in hydraulic head is equal to the topographic gradient.

A further addition to JULES that is used here is a river routing model (Bell et al., 2007; Dadson et al., 2011), which directs runoff produced by JULES into a channel network derived from a DEM. The model is based on an explicit finite difference approximation to the 1-D kinematic wave equation using 0.5° resolution flow paths constructed by applying the algorithm of da Paz et al. (2011) to HydroSHEDS topographic data produced by Lehner et al. (2008). Routing is applied separately using different wave speeds to surface and subsurface hillslope runoff components as well as open and subsurface channel flow (Bell and Moore, 1998). A return flow term accounts for interaction between surface and subsurface components.

2.2 Data sets and catchments

The input variables required to drive JULES – namely rainfall rate, air temperature at 2 m, specific humidity at 2 m, surface pressure, wind speed at 10 m, and surface downward long- and shortwave radiation – are provided by the WATCH Forcing Data (WFD; Weedon et al., 2011). The WFD were created by interpolating the ERA-40 reanalysis (Uppala et al., 2005) onto a 0.5° grid over the land surface and correcting for biases according to observed data sets. Monthly precipitation totals were corrected to match the Global Precipitation Climatology Centre (GPCC) product (Schneider et al., 2013) and number of wet days in each month were adjusted toward Climatic Research Unit (CRU) TS2.1 observations (Mitchell and Jones, 2005). Full details of the procedure are given in Weedon et al. (2011). The period January 1981 to December 2002 has been chosen for the JULES simulations to coincide with the period for which the maximum common length of river flow observations is available.

11099

An updated version of the WFD based on the ERA-Interim reanalysis has recently been released. We compared monthly climatologies between the two products for our study catchments and found differences of up to 10 % in the summer months in the upper Orange, but very slight differences for the Okavango and Zambezi subcatchments (not shown). An important caveat for both WFD sets is that the observed rainfall fields used to nudge the reanalysis suffer from poor station coverage for much of the region. Angola and western Zambia, for example, where the headwaters of the Okavango and Zambezi originate, are extremely data-poor areas. Uncertainty associated with rainfall estimates in this area is therefore high and biases are likely to be introduced into hydrological simulations. An alternative to station-dependant rainfall measurements is satellite-derived products, but these have their own caveats and biases. For example, Li et al. (2013) compared the WFD with the Tropical Rainfall Measuring Mission (TRMM) product (Huffman et al., 2007) and found an extensive underestimation of TRMM vs. WFD for the period 1997–2001 over Angola, northern Namibia and most of Zambia of over 100 mm yr^{-1} (see their Fig. 3). Li et al. (2013) do, however, find that runoff simulated by a hydrological model in this region is higher for TRMM than for WFD, which suggests that differences in rainfall intensity between the two products at daily and sub-daily time scales may be an important consideration here.

Observed daily and monthly river flow data for 3 stations on the Orange, Okavango and Zambezi rivers were obtained from the Global Runoff Data Centre, 56 068 Koblenz, Germany. Although more stations are available for these rivers we only present results here for Aliwal North on the Orange, Mohembo on the Okavango and Katima Mulilo on the Zambezi. The reason for selecting these stations is that the river channels upstream from these sites are relatively unmodified by large dams or excessive abstraction. The exception is Aliwal North, where the flow may be modified to some degree by the Lesotho Highlands Water Transfer Scheme, but this program has only come online in the late 1990s and investigation of the observed flow for the latter years of the simulation period reveals no significant change in runoff amount or runoff/rainfall ratio.

11100

Figure 1 displays the locations of the 3 discharge stations and the upstream catchment masks as defined in the JULES domain.

Of particular interest for the selected catchments is the contrasting geological environments represented. The contrast is most evident between the upper Orange section, which is characterised by steep-sloped mountainous terrain and moderate to deep clayey soils (Middleton and Bailey, 2009) and the Okavango headwaters, which are mostly underlain by thick deposits of Kalahari sand that have a very high infiltration capacity and porosity (Mendelsohn et al., 2009). Recharge into subsurface layers in the Okavango is therefore high and river discharge is dominated by a large baseflow component.

JULES evapotranspiration (ET) output is compared to the MOD16 data set of Mu et al. (2011). The MOD16 ET algorithm is based on the Penman–Monteith equation and uses a combination of inputs from satellite derived land-surface fields and meteorological reanalysis data. The comparison between JULES and MOD16 essentially compares two model estimates of ET, rather than a model vs. observation, but this nevertheless gives an indication of possible biases in the JULES output. The data are only available from 2000–2010, so only the final 2 yr of the JULES simulations are evaluated.

2.3 Model simulations

JULES has been configured for a domain covering the Southern African continental land surface south of the equator. The grid resolution is 0.5° , which corresponds to that of the WFD driving fields. Various simulations were run for the period 1981 to 2001 to test different model configurations and parameter sensitivities. Both the PDM and TOPMODEL sub-grid parameterization schemes were implemented and for comparison a simulation was also done where no sub-grid runoff scheme was used. Initial experiments identified that river discharge simulated by the PDM scheme is highly sensitive to the b shape parameter and that TOPMODEL is most sensitive to the f exponent (see Sect. 2.1). The following parameter settings are presented here to illustrate

11101

these sensitivities: PDM with $b = 0.1$ and $b = 0.3$ (hereafter referred to as PDM0.1 and PDM0.3, respectively) and TOPMODEL with $f = 0.5$, $f = 1.0$ and $f = 2.0$ (TOP0.5, TOP1.0 and TOP2.0, respectively). These parameters are constant across the model domain and their values are within the range of previous regional implementations of the respective schemes. This is discussed further in Sect. 4.

For the TOPMODEL configurations, values for the mean and standard deviation of the topographical index (TI) are supplied as a spatially-varying ancillary field. Further tests were also carried out to assess sensitivity to parameters in the river routing scheme. There are 4 parameters defining the wave speeds of the surface and sub-surface flow components for land and open channel grid points, respectively. A further parameter specifies the proportion of return flow from the subsurface to surface routing channels. Two additional simulations are presented here in which $f = 1.0$ and (a) all flow speed parameters are substantially reduced (TOP1.0c) and (b) flow speed parameters are reduced and the return flow parameter is increased (TOP1.0cr). A reference simulation is also presented, in which no sub-grid runoff parameterisation scheme is used (NO_SG). In NO_SG, surface runoff is produced by JULES in the form of infiltration excess at the grid point scale, but there is no representation of saturation excess overland flow or sub-grid heterogeneity. Table 1 summarises the different parameter settings for the simulations.

Three performance metrics are used to assess the efficacy of the model simulated monthly mean river discharge. The percentage error in mean discharge dQ is defined as

$$dQ = 100 \left[\frac{\bar{P} - \bar{O}}{\bar{O}} \right] \quad (3)$$

where P and O are modelled and observed discharge, respectively, and bars denote averages over the full simulation period. The Nash–Sutcliffe efficiency statistic E (Nash and Sutcliffe, 1970) is calculated as

11102

$$E = 1.0 - \frac{\sum_{i=1}^n (O_i - P_i)^2}{\sum_{i=1}^n (O_i - \bar{O})^2} \quad (4)$$

where n is the number of months and O_i and P_i are observed and modelled discharge for each month. Root mean square error RMSE is calculated as

$$\text{RMSE} = \sqrt{\frac{1}{n} \sum_{i=1}^n (O_i - P_i)^2} \quad (5)$$

3 Results

3.1 River flow

Figures 2–4 show monthly mean climatologies of JULES simulated river flow compared against discharge observations for the 3 selected subcatchments. The dashed curve represents observed flow at the relevant GRDC station and the solid curves show simulated river flow from the various JULES sensitivity tests at the grid point corresponding to the station location. Precipitation from the WFD is displayed as bars.

For the upper Orange catchment, measured at Aliwal North (Fig. 2), it is seen that observed river flow has a very fast response to rainfall. This is consistent with the geology of the catchment, which is characterised by steep-sloped mountainous terrain and moderate to deep clayey soils (Middleton and Bailey, 2009). A close match to the observations is given by PDM0.3, where $dQ = 8.4\%$ and $E = 0.77$ (Table 2). However, the large sensitivity to b is clearly shown: as b is reduced from 0.3 (PDM0.3) to 0.1 (PDM0.1) the mean annual discharge decreases from $\sim 165 \text{ m}^3 \text{ s}^{-1}$ to $\sim 85 \text{ m}^3 \text{ s}^{-1}$, and peak flow in February is reduced from $\sim 330 \text{ m}^3 \text{ s}^{-1}$ to $\sim 180 \text{ m}^3 \text{ s}^{-1}$. A higher value for

11103

b means that there is a relatively high proportion of shallow soil water stores compared to deep stores within a grid box. This is consistent with the physical environment of this catchment and so the PDM scheme does well in representing the river flow here. Very different results are produced by JULES when no sub-grid parameterization is used (NO_SG) and when TOPMODEL is implemented. For NO_SG, peak flow occurs later (in March) and is much smaller than observed ($\sim 40 \text{ m}^3 \text{ s}^{-1}$ vs. $\sim 315 \text{ m}^3 \text{ s}^{-1}$). The TOPMODEL simulations produce more discharge than NO_SG, but still well below observed, peaking at less than $90 \text{ m}^3 \text{ s}^{-1}$ in March for TOP1.0cr. Little sensitivity to variations in the f parameter is demonstrated. TOP1.0c and TOP1.0cr result in a delayed timing of peak discharge and the latter results in a small increase in magnitude. The NO_SG and TOPMODEL configurations all produce values for E less than 0 and negative dQ values greater than $\sim 70\%$ (Table 2).

In the Okavango subcatchment (Fig. 3) the behaviour of JULES is considerably different from what is shown for the upper Orange. All PDM configurations result in peak discharge that is much too high and occurs too early in the year. There is also a very large difference in the magnitude of simulated flow for the different values of b . Observed peak flow of $\sim 420 \text{ m}^3 \text{ s}^{-1}$ occurs in April, whereas the most conservative PDM estimate (TOP0.1) is a peak of over $800 \text{ m}^3 \text{ s}^{-1}$ in March. The observed dry-season flow in the Okavango is relatively high because of a large amount of recharge into the stream channel from slow sub-surface runoff. This dry-season flow is absent in the PDM simulations. In the NO_SG simulation, peak flow occurs a month late (in May) and its magnitude is about half that of observed. Dry-season flow is also largely absent in the NO_SG configuration. The sensitivity of the TOPMODEL simulations to changes in f are considerable. As f is decreased in TOPMODEL, so the rate of decay of K_{sat} in the deep soil layer decreases and hence subsurface runoff increases. This is reflected in the results, where both peak flow and dry-season flow increase with decreasing f . Peak discharge ranges from $\sim 480 \text{ m}^3 \text{ s}^{-1}$ for TOP2.0 to $\sim 580 \text{ m}^3 \text{ s}^{-1}$ for TOP0.5. Timing of the peak flow is too early for TOP0.5 and TOP1.0 (occurring in February), but matches observations for TOP2.0. The early timing of peak discharge is corrected by reducing

11104

the wave speed parameters in the routing module (TOP1.0c). This configuration yields the closest match to observations in terms of E (-0.62) and RMSE (162.4), but wet (dry) season discharge is overestimated (underestimated). Increasing return flow from the subsurface routing channel (TOP1.0cr) enhances wet season discharge, but has negligible effect in the dry season. None of the configurations tested result in a positive value for E (Table 3). The lowest annual bias is given by TOP1.0 ($dQ = 8.4\%$), but seasonal characteristics for this run are not accurately simulated.

Simulations for the upper reaches of the Zambezi, measured at Katima Mulilo (Fig. 4) show similar results to those of the Okavango. PDM overestimates peak flow, albeit by not as much as in the Okavango, and does not replicate observed dry-season flow. TOP0.5, TOP1.0 and TOP2.0 simulate peak flow one to two months too early, with the latter producing the lowest annual bias ($dQ = 7.2$; Table 4). However TOP2.0 does not replicate well the dry season discharge. Seasonal timing is improved by reducing the wave speed parameters (TOP1.0c) which yields the best E (0.61) but discharge is overestimated for most months, resulting in a bias of $dQ = 34.7\%$.

3.2 Grid point runoff

For a closer look at how available water is partitioned between surface and subsurface components for different parameter settings, two grid points have been selected, one in the upper Orange catchment (Fig. 5) and one in the headwaters of the Okavango (Fig. 6). These results help to diagnose where biases in the catchment-wide discharge originate in the model before the river routing scheme is invoked. Two PDM runs (PDM0.3 and PDM0.1) and three TOPMODEL configurations (TOP0.5, TOP1.0 and TOP2.0) are shown.

Runoff at the grid point in the upper Orange catchment (Fig. 5) is dominated by the surface component, with the portion of runoff occurring below the surface smaller by an order of magnitude. This is consistent with the “flashy” nature of this mountainous catchment. For the PDM runs, increased b results in substantially increased surface runoff as the relative proportion of small soil stores increases. This is accompanied by

11105

a corresponding along with a corresponding reduction in the subsurface runoff component. The net increase in runoff is balanced by reduced ET, as shown by the P -ET plot (Fig. 5a) and a reduction in total soil moisture content (SMC; Fig. 5d). Relatively large decreases in subsurface runoff are shown throughout the year for increasing values of f in the TOPMODEL configurations. Wet-season surface runoff decreases by increasing f from 1.0 to 2.0, but increasing f from 0.5 to 1.0 actually increases surface runoff slightly, indicating a non-linear sensitivity to this parameter.

For the Okavango grid point (Fig. 6), a similar sensitivity to b is shown for surface runoff in the PDM runs. Large increases in surface runoff in response to increased b are accompanied by reduced subsurface runoff from February to May. The magnitude of the subsurface component is a greater proportion of total runoff here than for the upper Orange, which is consistent with the deep, sandy soil profile characteristic of the Okavango headwaters. Relatively small changes in surface runoff result from varying the TOPMODEL f , but the subsurface component exhibits some interesting behaviour. TOP0.5 and TOP2.0 have similar curves, but the former is more delayed with higher runoff occurring from April to July, but slightly lower in February. TOP1.0, however, produces considerably less subsurface runoff from February to May, but more from July to December. This change in the seasonal distribution of subsurface runoff is an important consideration for the Okavango catchment and is discussed further in Sect. 4. The differences in total runoff between the simulations are balanced by changes in ET that occur during the dry season, when evaporative demand exceeds rainfall, and changes in SMC throughout the year.

3.3 Evapotranspiration

Comparison of JULES ET against the MOD16 product are made for the years 2000 and 2001. Monthly ET is averaged over the three subcatchments and presented for the “best” JULES configurations as per the performance metrics. The aim of this is to give an indication of biases inherent in JULES ET, rather than test the sensitivity of the modelled ET to parameter changes. For the upper Orange catchment (Fig. 7), a large

11106

overestimation of ET is given by JULES, showing more than double the MOD16 estimate for most months. The tendency for JULES to simulate excessive ET in this catchment is also seen in the TOPMODEL configurations (not shown), indicating that the ET overestimate is independent of runoff production scheme. In the Okavango catchment upstream from Mohembo (Fig. 8), JULES simulates a seasonal cycle of greater amplitude than MOD16, with peak rates in the late summer months overestimated by more than 20 mm month⁻¹. Dry season ET minimum is underestimated by the model and occurs later in the year than MOD16. This pattern is similar for the Zambezi upstream from Katima Mulilo (Fig. 9), except that the seasonal minimum is not underestimated by JULES, but rather delayed by 2–3 months.

4 Discussion

The PDM runoff production scheme performs best for the upper Orange catchment, where simulated river discharge can be scaled by varying the b parameter and a very good agreement with observed river flow can thus be obtained. In the Okavango and Zambezi catchments, however, PDM overestimates annual stream flow by > 30% for values of $b = 0.1$ and > 90% for $b = 0.3$. Reynard et al. (1997) implemented a PDM-based rainfall-runoff model for Southern Africa in which they set b to a global value of 0.25. Using rainfall input from the Climatic Research Unit (CRU) gridded observations, their simulations resulted in good correlation to observed annual runoff time series for 1961–1990, but a systematic overestimation of mean annual runoff for the domain (Reynard et al., 1997). It is likely that their overall runoff bias could be reduced by using a smaller b value, but our results show that a single domain-wide b value is not appropriate to capture correctly annual stream flow magnitude for individual catchments in the domain. In order to overcome this, Dadson et al. (2011) derived a spatially variable field for the PDM b parameter from soil depth data for Europe, where values for b were constrained between 0 and 1. A similar approach could be attempted for Southern Africa given reliable soil data.

11107

In contrast to PDM, the TOPMODEL scheme performs very poorly in the upper Orange catchment as it grossly underestimates discharge. The reduced runoff is balanced by an increase in ET. In the Okavango and Zambezi catchments, TOPMODEL performs better in that it can be tuned to produce realistic dry-season flow, but wet-season discharge remains excessive. The timing of the seasonal peak can be adjusted by tuning the parameters in the river routing scheme that control the wave speeds of subsurface runoff components. This solution does not, however, have a physical basis in that although it improves model performance, it does not account for the cause of the discrepancy. Analyses of the available archival discharge data from the Okavango indicate that discharge peak occurs late in the rainy season (March) even in relatively small upstream catchments, where the role of river valley storage, and hence the wave delay, is minimal.

The values for the TOPMODEL f parameter that produces the lowest bias in mean annual discharge differs between the Okavango and Zambezi (1.0 and 2.0 respectively). These values are higher than that used by Gedney and Cox (2003), who found that $f = 0.5$ yielded an optimum global mean annual runoff to precipitation ratio for an implementation of TOPMODEL in the MOSES LSM with rainfall input from Xie and Arkin (1997). This global parameter setting does of course not account for inter-catchment variability and our work suggests that realistic simulations cannot be achieved unless this spatial variability is accounted for. One way to achieve this could be to derive a spatially varying field for f as a function of some other physical property such as soil depth or texture. This has not been addressed in the current paper, but should fall under the scope of future work.

A major inadequacy of the JULES PDM configuration is that it cannot replicate the dry-season flow that is a prominent feature of the Okavango and Zambezi rivers. The eastern headwaters of the Okavango, in particular, are underlain by thick deposits of Kalahari sand which have a very high infiltration capacity and porosity (Mendelsohn et al., 2009). Recharge into subsurface layers is therefore high and river discharge is dominated by a high baseflow component, which contributes about 70% of peak

11108

monthly discharge (Hughes et al., 2004). Because this subsurface flow occurs slowly, it can persist for months to years, which dampens seasonal and interannual variability. At the seasonal time scale, the difference between PDM and TOPMODEL simulations of subsurface runoff is stark (Fig. 6c). PDM produces a strong peak in February and negligible runoff during the dry season (June to December), whereas TOPMODEL has a delayed peak in March and persistent runoff throughout the dry season. The latter is clearly a more realistic representation of typical Okavango hydrology. The interannual effect of slow baseflow recharge is seen in correlations between mean annual time series of JULES simulated discharge for the Okavango at Mohembo and rainfall input for the upstream catchment for 1981–2001. For TOPMODEL (run TOP1.0c), the correlation coefficient of $r = 0.38$ reveals weak coupling between interannual variations in rainfall and river discharge, which is consistent with a baseflow-controlled catchment. PDM (run PDM0.1), on the other hand, has a substantially higher correlation of $r = 0.55$, indicating a weaker effect of the slow baseflow component. Therefore at both seasonal and interannual time scales TOPMODEL provides more realistic simulations, but still suffers from a positive bias in wet season discharge. This bias could be explained partly by three factors: (1) bias in rainfall input due to poor station coverage in the catchment, (2) transmission losses that are not accounted for by JULES and (3) underestimation of the surface/subsurface runoff partitioning. The second factor is most relevant in the lower parts of the catchment, where progressively lower rainfall, deep sandy soils and a poorly developed surface drainage network actually result in river flow decreasing in the downstream direction (Hughes et al., 2004). The third factor may be of importance if in reality the role of infiltration to groundwater and thus subsurface runoff is larger than that obtained with the model structure and tested parameterization. Interestingly, an increase in the role of infiltration and subsurface runoff would help account for other discrepancies in the model output, i.e. earlier than observed timing of the peak runoff and underestimation of dry season discharges. Unfortunately, the lack of water balance studies in the Okavango headwaters prevents a detailed elaboration on the significance of this potential source of model bias.

11109

The major shortcoming of TOPMODEL in the upper Orange catchment is its gross underestimation of river flow magnitude. A possible cause of this is inappropriate topographical index ancillary data. In the test configurations presented in this study we do not alter the topographical index (TI) values given by the ancillary data, but additional tests were run (not shown) to investigate sensitivities to the TI. It was found that the magnitude of saturation excess surface runoff is substantially increased by increasing gridbox mean TI. A new TI data set is currently under preparation and comparison between a preliminary version of this and the current ancillary field shows higher TI values over much of the upper Orange basin (not shown), which suggests potential for improved surface runoff simulation in TOPMODEL for this catchment. It is also noteworthy that all simulations in the upper Orange produce an overestimation of ET when compared to the MOD16 estimate. If the MOD16 estimate is reliable for this location, this implies that although the PDM0.3 configuration results in a good match to observed discharge, the water balance over the catchment is fact incorrectly represented. The causes of this ET overestimation need to be investigated in more detail, but a possible explanation is excessive soil moisture storage by JULES. Since JULES does not allow for a spatially-variable soil column depth, it is plausible that in a catchment such as the upper Orange, where soils are relatively shallow, the model allows too great a quantity of water to be stored in the soil column. This would explain the overestimation of ET by all JULES configurations tested here as more water is available in the root zone for transpiration. Furthermore, an excessively deep soil column could also explain the underestimation of runoff by TOPMODEL as more water can be stored before the soil becomes saturated and runoff is produced. Further work is required to test this hypothesis by examining different soil profiles in JULES and evaluating simulated soil moisture against observations.

11110

5 Conclusions

This study has tested the JULES LSM over a Southern African domain to determine sensitivity to model configuration and parameter settings. Particular focus has been given to simulated river discharge in the upper reaches of the Orange, Okavango and Zambezi catchments. The comparison between the upper Orange, with its steep topography and relatively shallow soils, and the Okavango and Zambezi, where deep sandy soil profiles dominate, provides some interesting insight into how JULES behaves in contrasting physical environments. The PDM runoff generation scheme performs best in the upper Orange catchment, but does a poor job in replicating the magnitude and timing of runoff and discharge in the Okavango and Zambezi. TOPMODEL grossly underestimates the magnitude of discharge in the upper Orange, but performs better in the Okavango and Zambezi as it provides an improved representation of subsurface runoff to the stream flow.

The results presented here show that there is not a single optimal model configuration for the region, but different catchments are suited to different runoff schemes and parameter settings. There is nevertheless scope to introduce greater spatial heterogeneity in parameter data sets in order to work towards a regionally optimum model configuration. Since subsurface flow is a very important feature of the Okavango and Zambezi catchments, we would argue that TOPMODEL is a better choice than PDM in this region. Further work is needed to understand why, in the present study, TOPMODEL performs poorly in representing the magnitude of stream flow in fast-runoff environments similar to the upper Orange.

Acknowledgements. We are grateful for support provided through the knowledge exchange component of the NERC funded project “Changing Land–Atmosphere Feedbacks in Tropical African Wetlands” (NE/I01 277X/1) to enable the first author to spend time at the Oxford University Centre for the Environment during 2012. We also thank T. Marthews, R. Ellis, N. Gedney and D. Clark for valuable comments and technical assistance with JULES. River discharge data were provided by the Global Runoff Data Centre, 56 068 Koblenz, Germany.

11111

References

- Alkama, R., Decharme, B., Douville, H., Becker, M., Cazenave, A., Sheffield, J., Voldoire, A., Tyteca, S., and Le Moigne, P.: Global evaluation of the ISBA-TRIP continental hydrological system: Part I. Comparison to GRACE terrestrial water storage estimates and in situ river discharges, *J. Hydrometeorol.*, 11, 583–600, 2010.
- Arnell, N. W.: Climate change and global water resources: SRES emissions and socio-economic scenarios, *Global Environ. Chang.*, 14, 31–52, 2004.
- Bell, V. A. and Moore, R. J.: A grid-based distributed flood forecasting model for use with weather radar data: Part 1. Formulation, *Hydrol. Earth Syst. Sci.*, 2, 265–281, doi:10.5194/hess-2-265-1998, 1998.
- Bell, V. A., Kay, A. L., Jones, R. G., and Moore, R. J.: Use of a grid-based hydrological model and regional climate model outputs to assess changing flood risk, *Int. J. Climatol.*, 27, 1657–1671, 2007.
- Best, M. J., Pryor, M., Clark, D. B., Rooney, G. G., Essery, R. L. H., Ménard, C. B., Edwards, J. M., Hendry, M. A., Porson, A., Gedney, N., Mercado, L. M., Sitch, S., Blyth, E., Boucher, O., Cox, P. M., Grimmond, C. S. B., and Harding, R. J.: The Joint UK Land Environment Simulator (JULES), model description – Part 1: Energy and water fluxes, *Geosci. Model Dev.*, 4, 677–699, doi:10.5194/gmd-4-677-2011, 2011.
- Beven, K.: TOPMODEL: A critique, *Hydrol. Process.*, 11, 1069–1085, 1997.
- Beven, K.: A manifesto for the equifinality thesis, *J. Hydrol.*, 320, 18–36, 2006.
- Beven, K. and Freer, J.: Equifinality, data assimilation, and uncertainty estimation in mechanistic modelling of complex environmental systems using the GLUE methodology, *J. Hydrol.*, 249, 11–29, 2001.
- Beven, K. J. and Kirkby, M. J.: A physically based, variable contributing area model of basin hydrology, *Hydrological Sciences Bulletin*, 24, 43–69, 1979.
- Beven, K. J., Lamb, R., Quinn, P., Romanowicz, R., and Freer, J.: TOPMODEL, in: *Computer Models of Watershed Hydrology*, edited by: Singh, V. P., Water Resource Publications, Colorado, 627 pp., 1995.
- Brooks, R. H. and Corey, A. T.: Hydraulic properties of porous media, *Hydrology Papers*, Colorado State University, 1964.

11112

- Clark, D. B. and Gedney, N.: Representing the effects of subgrid variability of soil moisture on runoff generation in a land surface mode, *J. Geophys. Res.*, 113, D10111, doi:10.1029/2007JD008940, 2008.
- Clark, D. B., Mercado, L. M., Sitch, S., Jones, C. D., Gedney, N., Best, M. J., Pryor, M., Rooney, G. G., Essery, R. L. H., Blyth, E., Boucher, O., Harding, R. J., Huntingford, C., and Cox, P. M.: The Joint UK Land Environment Simulator (JULES), model description – Part 2: Carbon fluxes and vegetation dynamics, *Geosci. Model Dev.*, 4, 701–722, doi:10.5194/gmd-4-701-2011, 2011.
- Cox, P. M., Betts, R. A., Bunton, C. B., Essery, R. L. H., Rowntree, P. R., and Smith, J.: The impact of new land surface physics on the GCM simulation of climate and climate sensitivity, *Clim. Dynam.*, 15, 183–203, 1999.
- da Paz, A. R., Collischonn, W., Tucci, C. E. M., and Padovani, C. R.: Large-scale modelling of channel flow and floodplain inundation dynamics and its application to the Pantanal (Brazil), *Hydrol. Process.*, 25, 1498–1516, 2011.
- Dadson, S. J., Bell, V. A., and Jones, R. G.: Evaluation of a grid-based river flow model configured for use in a regional climate model, *J. Hydrol.*, 411, 238–250, 2011.
- De Wit, M. and Stankiewicz, J.: Changes in surface water supply across africa with predicted climate change, *Science*, 311, 1917–1921, 2006.
- Essery, R. L. H., Best, M. J., Betts, R. A., Cox, P. M., and Taylor, C. M.: Explicit representation of subgrid heterogeneity in a GCM land surface scheme, *J. Hydrometeorol.*, 4, 530–543, 2003.
- Gedney, N. and Cox, P. M.: The sensitivity of global climate model simulations to the representation of soil moisture heterogeneity, *J. Hydrometeorol.*, 4, 1265–1275, 2003.
- Hagemann, S. and Dümenil, L.: A parametrization of the lateral waterflow for the global scale, *Clim. Dynam.*, 14, 17–31, 1998.
- Hughes, D. A.: Incorporating groundwater recharge and discharge functions into an existing monthly rainfall–runoff model, *Hydrolog. Sci. J.*, 49, 297–311, doi:10.1623/hysj.49.2.297.34834, 2004.
- Lehner, B., Verdin, K., and Jarvis, A.: New global hydrography derived from spaceborne elevation data, *EOS T. Am. Geophys. Un.*, 89, 93–94, 2008.
- Li, L., Ngongondo, C. S., Xu, C. Y., and Gong, L.: Comparison of the global TRMM and WFD precipitation datasets in driving a large-scale hydrological model in Southern Africa, *Hydrol. Res.*, 10, online first, doi:10.2166/nh.2012.175, 2013.

11113

- Meigh, J., McKenzie, A., and Sene, K.: A grid-based approach to water scarcity estimates in eastern and southern Africa, *Water Resour. Manage.*, 13, 85–115, 1999.
- Mendelsohn, J. M., Vanderpost, C., Ramberg, L., Murray-Hudson, M., Wolski, P., and Mosepele, K.: Okavango Delta: floods of life, Harry Oppenheimer Okavango Research Centre, Maun, Botswana, 2010.
- Middleton, B. J. and Bailey, K.: Water Resources of Southern Africa, 2005 Study (WR2005), Water Research Commission Report Number TT 382/08, Pretoria, 2009.
- Miller, J. R., Russell, G. L., and Caliri, G.: Continental-scale river flow in climate models, *J. Climate*, 7, 914–928, 1994.
- Mitchell, T. D. and Jones, P. D.: An improved method of constructing a database of monthly climate observations and associated high-resolution grids, *Int. J. Climatol.*, 25, 693–712, 2005.
- Moore, R. J.: The probability-distributed principle and runoff production at point and basin scales, *Hydrolog. Sci. J.*, 30, 273–297, 1985.
- Mu, Q., Zhao, M., and Running, S. W.: Improvements to a MODIS global terrestrial evapotranspiration algorithm, *Remote Sens. Environ.*, 115, 1781–1800, 2011.
- Nash, J. E. and Sutcliffe, J. V.: River flow forecasting through conceptual models – Part I: A discussion of principles, *J. Hydrol.*, 10, 282–290, 1970.
- Oki, T., Nishimura, T., and Dirmeyer, P.: Assessment of annual runoff from land surface models using Total Runoff Integrating Pathways (TRIP), *J. Meteorol. Soc. Jpn.*, 77, 235–255, 1999.
- Reynard, N., Andrews, A., and Arnell, N.: The derivation of a runoff grid for Southern Africa for climate change impact analyses, FRIEND '97 – Regional Hydrology: concepts and Models for Sustainable Water Resource Management (Proceedings of the Postojna, Slovenia, Conference, September–October 1997). IAHS Publ. no. 246, 1997.
- Schneider, U., Becker, A., Finger, P., Meyer-Christoffer, A., Ziese, M., and Rudolf, B.: GPCP's new land surface precipitation climatology based on quality-controlled in situ data and its role in quantifying the global water cycle, *Theor. Appl. Climatol.*, online first, doi:10.1007/s00704-013-0860-x, 2013.
- Schulze, R. E.: Modelling hydrological responses to land use and climate change: a Southern African perspective, *AMBIO*, 29, 12–22, 2000.
- Uppala, S. M., Kållberg, P. W., Simmons, A. J., Andrae, U., Bechtold, V. D. C., Fiorino, M., Gibson, J. K., Haseler, J., Hernandez, A., Kelly, G. A., Li, X., Onogi, K., Saarinen, S., Sokka, N., Allan, R. P., Andersson, E., Arpe, K., Balmaseda, M. A., Beljaars, A. C. M., Berg, L. V. D.,

11114

- Bidlot, J., Bormann, N., Caires, S., Chevallier, F., Dethof, A., Dragosavac, M., Fisher, M., Fuentes, M., Hagemann, S., Hólm, E., Hoskins, B. J., Isaksen, L., Janssen, P. A. E. M., Jenne, R., McNally, A. P., Mahfouf, J.-F., Morcrette, J.-J., Rayner, N. A., Saunders, R. W., Simon, P., Sterl, A., Trenberth, K. E., Untch, A., Vasiljevic, D., Viterbo, P., and Woollen, J.:
 5 The ERA-40 re-analysis, *Q. J. Roy. Meteor. Soc.*, 131, 2961–3012, 2005.
- Vörösmarty, C. J.: Global water resources: vulnerability from climate change and population growth, *Science*, 289, 284–288, 2000.
- Weedon, G. P., Gomes, S., Viterbo, P., Shuttleworth, W. J., Blyth, E., Österle, H., Adam, J. C., Bellouin, N., Boucher, O., and Best, M.: Creation of the WATCH Forcing Data and its use to
 10 assess global and regional reference crop evaporation over land during the twentieth century, *J. Hydrometeorol.*, 12, 823–848, 2011.
- Xie, P. and Arkin, P. A.: Global precipitation: a 17 yr monthly analysis based on gauge observations, satellite estimates, and numerical model outputs, *B. Am. Meteorol. Soc.*, 78, 2539–2558, 1997.

11115

Table 1. Summary of JULES configurations. Parameter names are: PDM shape parameter (b), TOPMODEL f exponent (f), kinematic wave speed parameters for surface and subsurface river flow in river channel (criver and cbriver, respectively) and the same for land grid points (cland and cbland, respectively) and return flow from subsurface to surface components of the river channel (retr).

| Run | b | f | criver | cbriver | cland | cbland | retr |
|----------|-----|-----|--------|---------|-------|--------|---------|
| NO_SG | – | – | 0.375 | 0.15 | 0.15 | 0.1125 | 0.00068 |
| PDM0.3 | 0.3 | – | 0.375 | 0.15 | 0.15 | 0.1125 | 0.00068 |
| PDM0.1 | 0.1 | – | 0.375 | 0.15 | 0.15 | 0.1125 | 0.00068 |
| TOP0.5 | – | 0.5 | 0.375 | 0.15 | 0.15 | 0.1125 | 0.00068 |
| TOP1.0 | – | 1.0 | 0.375 | 0.15 | 0.15 | 0.1125 | 0.00068 |
| TOP2.0 | – | 2.0 | 0.375 | 0.15 | 0.15 | 0.1125 | 0.00068 |
| TOP1.0c | – | 1.0 | 0.15 | 0.08 | 0.08 | 0.08 | 0.00068 |
| TOP1.0cr | – | 1.0 | 0.15 | 0.08 | 0.08 | 0.08 | 0.01 |

11116

Table 2. Performance metrics for simulated river flow at Aliwal North: observed and modelled mean annual discharge (Q_{obs} and Q_{mod} , respectively), percentage error in mean annual discharge (dQ), efficiency (E) and root mean square error (RMSE). Numbers in bold are the best match to observations.

| Orange at Aliwal North | | | | | |
|------------------------|----------------|----------------|------------|-------------|-------------|
| Run | Q_{obs} (mm) | Q_{mod} (mm) | dQ (%) | E | RMSE |
| NO_SG | 151.7 | 16.8 | -88.9 | -0.31 | 227.9 |
| PDM0.3 | 151.7 | 164.5 | 8.4 | 0.77 | 96.4 |
| PDM0.1 | 151.7 | 85.7 | -43.5 | 0.44 | 149.1 |
| TOP0.5 | 151.7 | 33.7 | -77.8 | -0.11 | 209.8 |
| TOP1.0 | 151.7 | 34.1 | -77.5 | -0.10 | 209.5 |
| TOP2.0 | 151.7 | 27.9 | -81.6 | -0.16 | 214.4 |
| TOP1.0c | 151.7 | 38.4 | -74.7 | -0.13 | 211.8 |
| TOP1.0cr | 151.7 | 45.9 | -69.7 | -0.08 | 207.5 |

11117

Table 3. As for Table 2, but at Mohembo.

| Okavango at Mohembo | | | | | |
|---------------------|----------------|----------------|------------|--------------|--------------|
| Run | Q_{obs} (mm) | Q_{mod} (mm) | dQ (%) | E | RMSE |
| NO_SG | 235.5 | 68.7 | -70.8 | -1.78 | 212.5 |
| PDM0.3 | 235.5 | 532.5 | 126.3 | -27.95 | 685.5 |
| PDM0.1 | 235.5 | 307.3 | 30.6 | -5.41 | 322.5 |
| TOP0.5 | 235.5 | 255.3 | 8.5 | -1.49 | 201.1 |
| TOP1.0 | 235.5 | 255.0 | 8.4 | -1.36 | 195.6 |
| TOP2.0 | 235.5 | 187.9 | -20.1 | -0.95 | 177.8 |
| TOP1.0c | 235.5 | 273.6 | 16.3 | -0.62 | 162.4 |
| TOP1.0cr | 235.5 | 300.6 | 27.8 | -1.21 | 189.4 |

11118

Table 4. As for Table 2, but at Katima Kulilo.

| Zambezi at Katima Mulilo | | | | | |
|--------------------------|----------------|----------------|------------|-------------|--------------|
| Run | Q_{obs} (mm) | Q_{mod} (mm) | dQ (%) | E | RMSE |
| NO_SG | 923.1 | 451.9 | -51.0 | 0.28 | 798.6 |
| PDM0.3 | 923.1 | 1795.1 | 94.5 | -2.89 | 1864.1 |
| PDM0.1 | 923.1 | 1251.3 | 35.6 | 0.11 | 891.1 |
| TOP0.5 | 923.1 | 1348.3 | 46.1 | -0.44 | 1133.2 |
| TOP1.0 | 923.1 | 1169.2 | 26.7 | 0.01 | 939.1 |
| TOP2.0 | 923.1 | 989.7 | 7.2 | 0.39 | 739.4 |
| TOP1.0c | 923.1 | 1243.0 | 34.7 | 0.61 | 589.3 |
| TOP1.0cr | 923.1 | 1321.8 | 43.2 | 0.52 | 657.2 |

11119

JULES subcatchments and river gauge stations

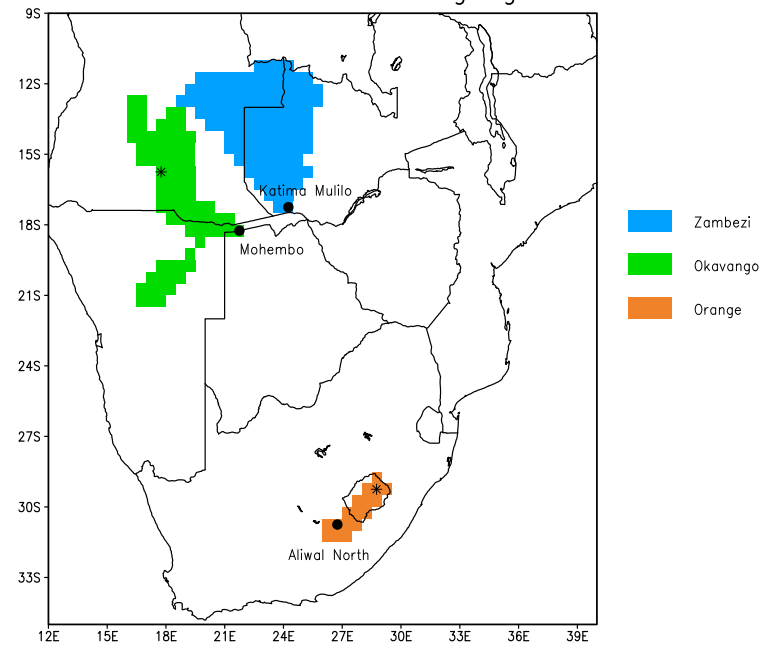


Fig. 1. Locations of GRDC discharge stations and JULES masks for the catchments areas upstream from these stations. Asterisks show locations of the grid points evaluated in Figs. 5 and 6.

11120

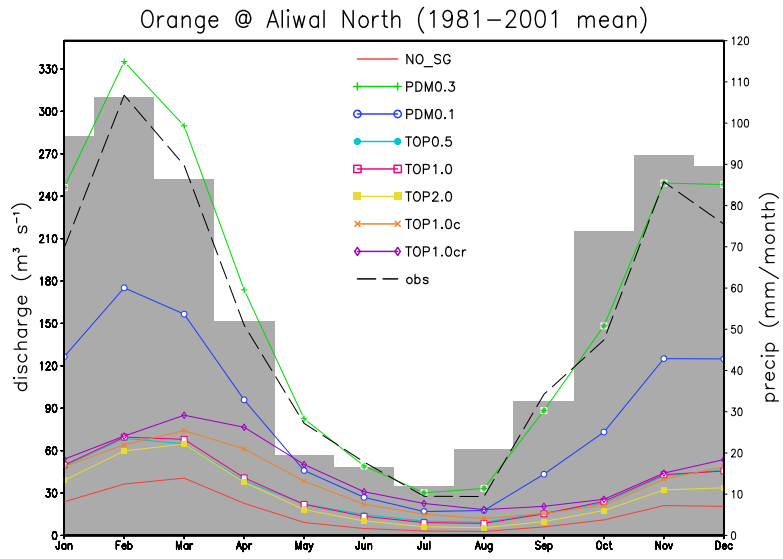


Fig. 2. Observed and simulated monthly river discharge for the Orange River at Aliwal North for 1981–2001. Bars represent WATCH Forcing Data rainfall, averaged over the area of the subcatchment.

11121

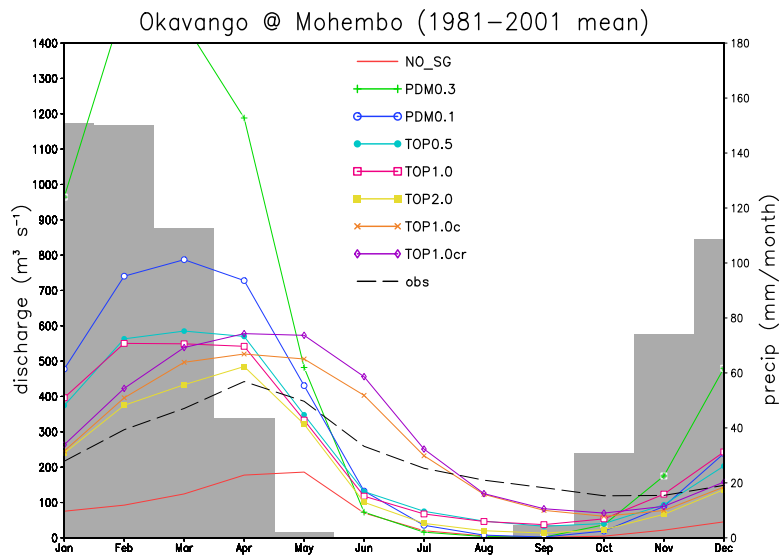


Fig. 3. As for Fig. 2, but for the Okavango at Mohembo.

11122

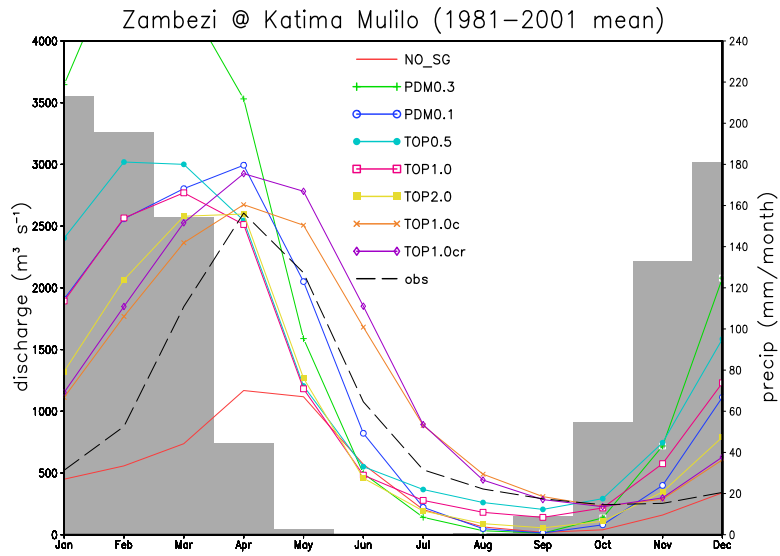


Fig. 4. As for Fig. 2, but for the Zambezi at Katima Mulilo.

11123

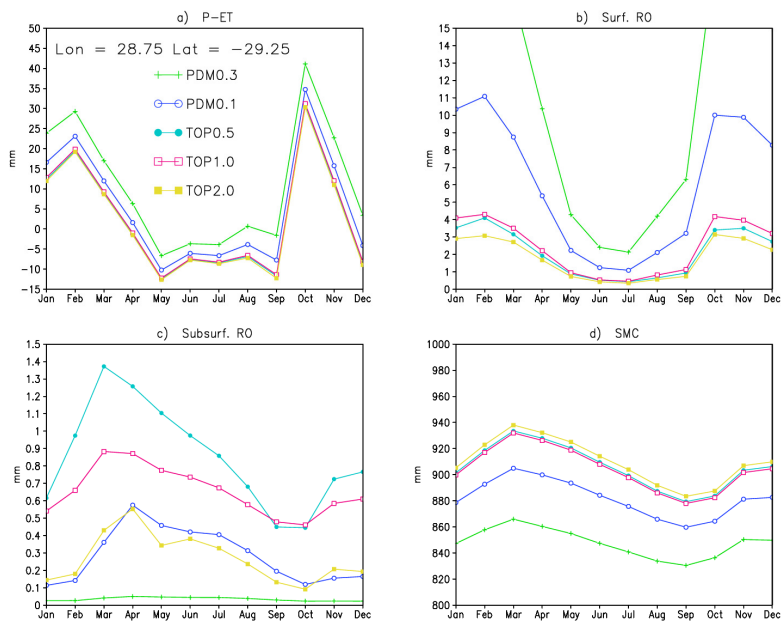


Fig. 5. Mean JULES outputs (averaged over 1981–2001) for (a) precipitation minus evapotranspiration, (b) surface runoff, (c) subsurface runoff and (d) total column soil water content for a single grid point located within the Orange catchment (longitude 28.75, latitude -29.25).

11124

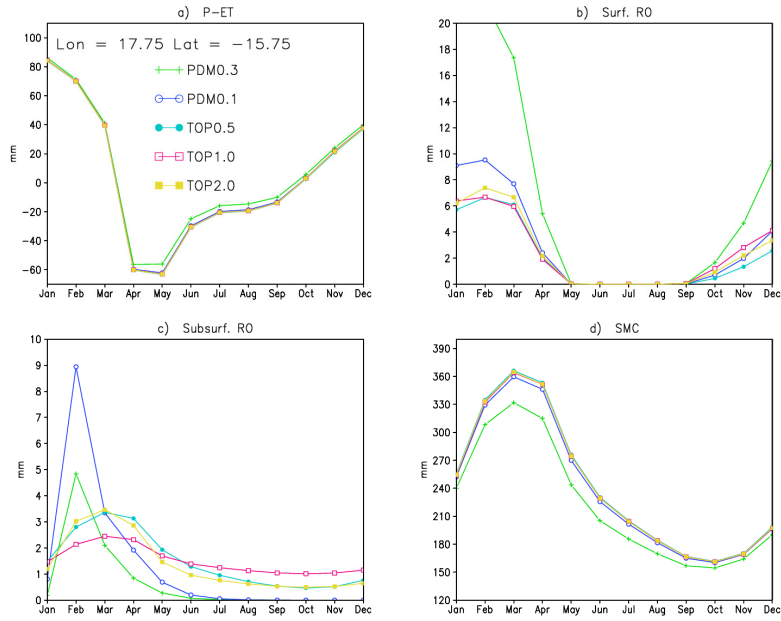


Fig. 6. as for Fig. 5, but for a single grid point in the Okavango catchment (longitude 17.75, latitude -15.75).

11125

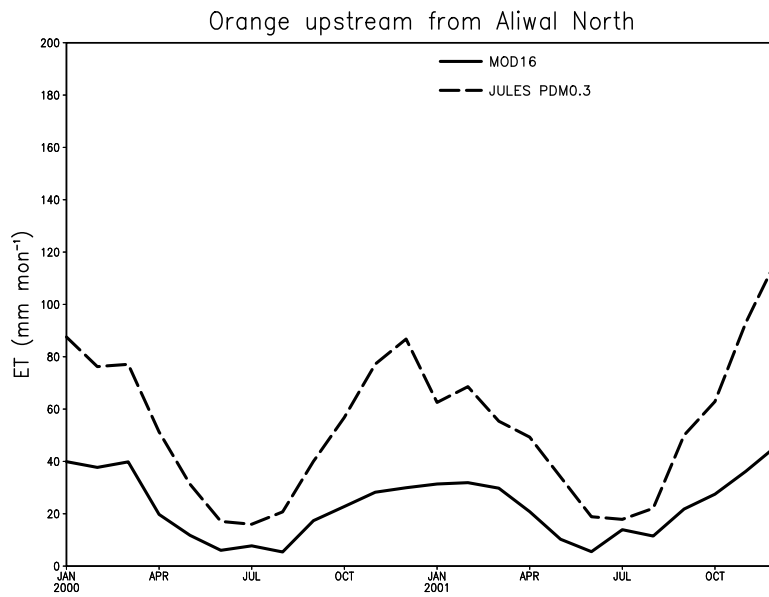


Fig. 7. JULES and MOD16 evapotranspiration averaged over the area of the Orange subcatchment.

11126

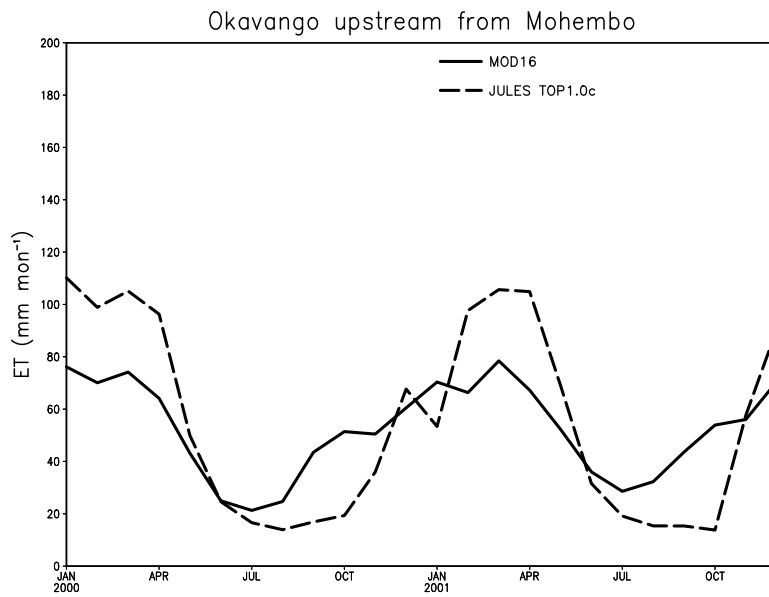


Fig. 8. As for Fig. 7, but for the Okavango subcatchment.

11127

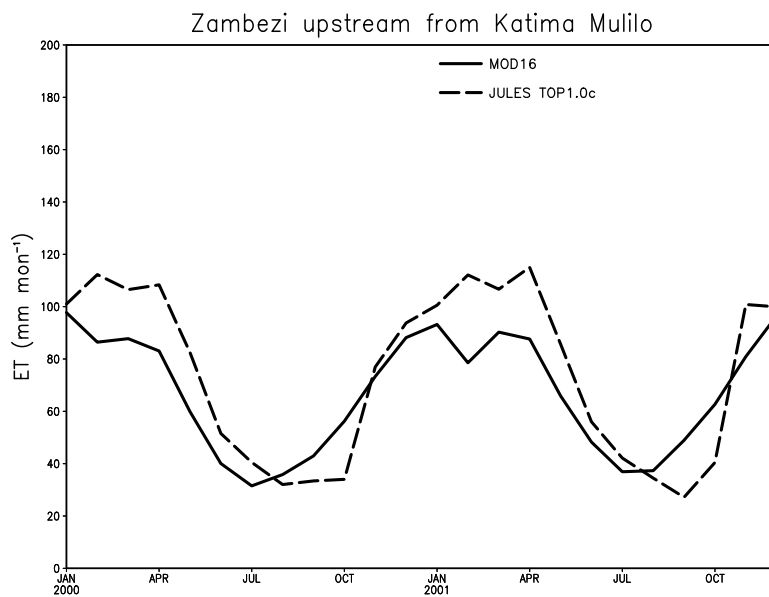


Fig. 9. As for Fig. 7, but for the Zambezi subcatchment.

11128